

Supporting Information for
One-pot synthesis of bi-metallic PdRu tripods as an efficient catalyst for
electrocatalytic nitrogen reduction to ammonia

Hongjing Wang, Yinghao Li, Chunjie Li, Kai Deng, Ziqiang Wang,* You Xu, Xiaonian Li,
Hairong Xue,* and Liang Wang*

State Key Laboratory Breeding Base of Green-Chemical Synthesis Technology, College of Chemical
Engineering, Zhejiang University of Technology, Hangzhou, Zhejiang 310014, P. R. China.

*Corresponding authors:

E-mails: zqwang@zjut.edu.cn; xuehairong@zjut.edu.cn; wangliang@zjut.edu.cn

Experimental Section

Determination of ammonia: The concentration of produced ammonia was determined by the indophenol blue method.¹ In detail, 2 mL aliquot of the electrolyte was received from the electrolytic cell, then mixed with 2 mL of 1 M NaOH solution containing salicylic acid (5 wt%) and sodium citrate (5 wt%). After that, 1 mL of 0.05 M NaClO and 0.2 mL of 1 wt % $C_5FeN_6Na_2O$ were added into the above solution. The ultraviolet-visible (UV-Vis) absorption spectrum (TU-1900) was measured after standing at room temperature for 2 h. The concentration of indophenol blue was determined using the absorbance at a wavelength of 655 nm. The concentration-absorbance curves were calibrated using standard ammonia chloride solution with a series of standard concentrations. The fitting curve ($y = 0.371x + 0.051$, $R^2 = 0.999$) shows good linear relation of absorbance value with NH_3 concentration.

Determination of hydrazine: The hydrazine presented in the electrolyte was estimated by the method of Watt and Chrisp.² A mixture of para-(dimethylamino) benzaldehyde (5.99 g), concentrated HCl (30 mL) and ethanol (300 mL) was used as a color reagent. In brief, 5 mL aliquot of the electrolyte was received from the electrolytic cell, then mixed with 5 mL color reagent. The UV-Vis absorption spectrum was measured after standing at room temperature for 10 min. The concentration was determined using the absorbance at a wavelength of 458 nm. The calibration curve of this method was achieved using hydrazine monohydrate solutions of known concentrations as standards, and the fitting curve shows good linear relation of absorbance with $N_2H_4 \cdot H_2O$ concentration ($y = 0.724x - 0.014$, $R^2 = 0.999$).

Calculation of double-layer capacitance: The electrochemically effective surface areas are reflected by double layer capacitances (C_{dl}), which can be calculated from cyclic voltammograms (CVs).³ CVs were performed at which no obvious Faradic current were

observed. The capacitive currents, $\Delta j/2$ ($\Delta j = j_a - j_c$, j_a and j_c refer to anodic and cathodic current densities at 0.42 V), were plotted against the scan rates between 20 and 100 mV s⁻¹.

The linear relationships were observed with the slope of the C_{dl} value.

Reference

1. D. Zhu, L. Zhang, R. E. Ruther and R. J. Hamers, *Nat. Mater.*, 2013, **12**, 836-841.
2. G. W. Watt and J. D. Chrisp, *Anal. Chem.*, 1952, **24**, 2006-2008.
3. Z. Wang, Z. Liu, G. Du, A. M. Asiri, L. Wang, X. Li, H. Wang, X. Sun, L. Chen and Q. Zhang, *Chem. Commun.*, 2018, **54**, 810-813.

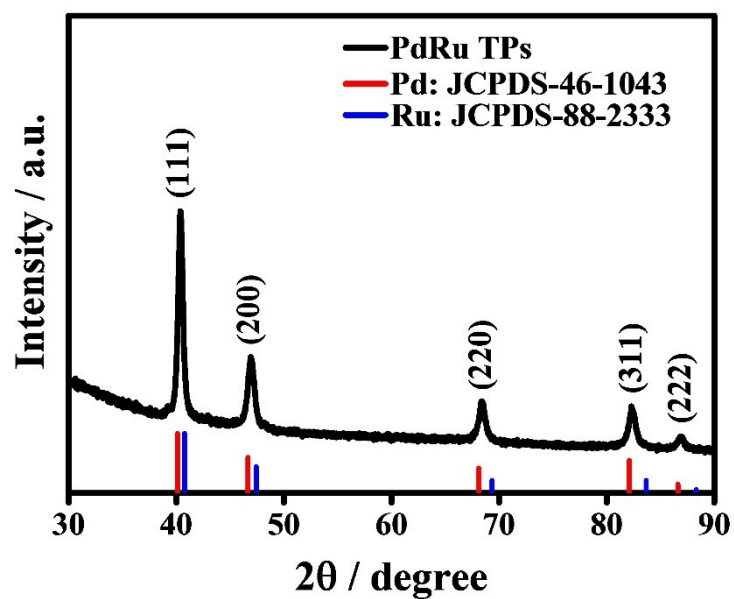


Fig. S1 XRD pattern of the PdRu TPs.

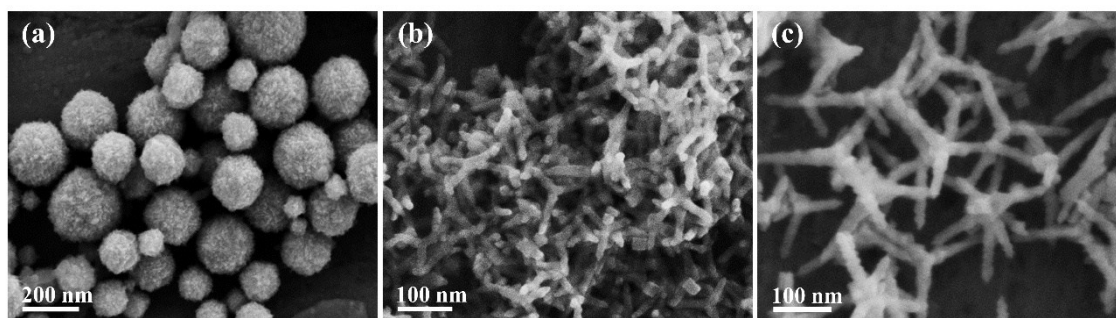


Fig. S2 SEM images of the samples prepared with different amounts of KBr: (a) 0 mg, (b) 10 mg, and (c) 160 mg.

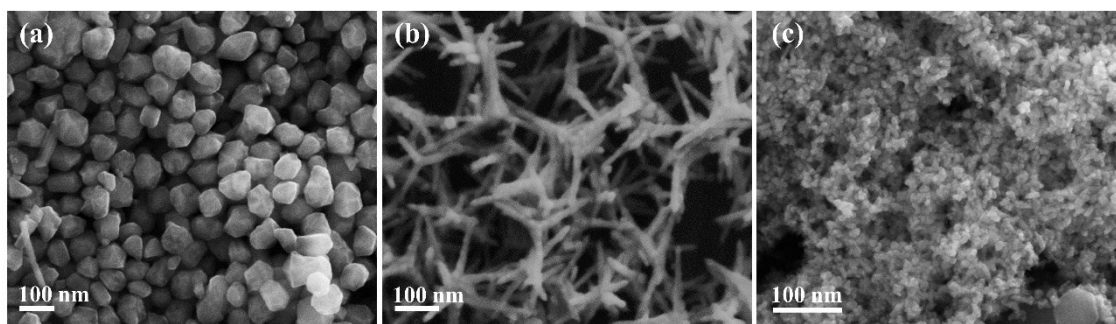


Fig. S3 SEM images of the PdRu samples prepared with different amounts of metallic precursor under the identical synthesis conditions: (a) Na_2PdCl_4 (3 mL, 20 mM), RuCl_3 (0 mL, 20 mM); (b) Na_2PdCl_4 (0.6 mL, 20 mM), RuCl_3 (2.4 mL, 20 mM); and (c) Na_2PdCl_4 (0.1 mL, 20 mM), RuCl_3 (2.9 mL, 20 mM).

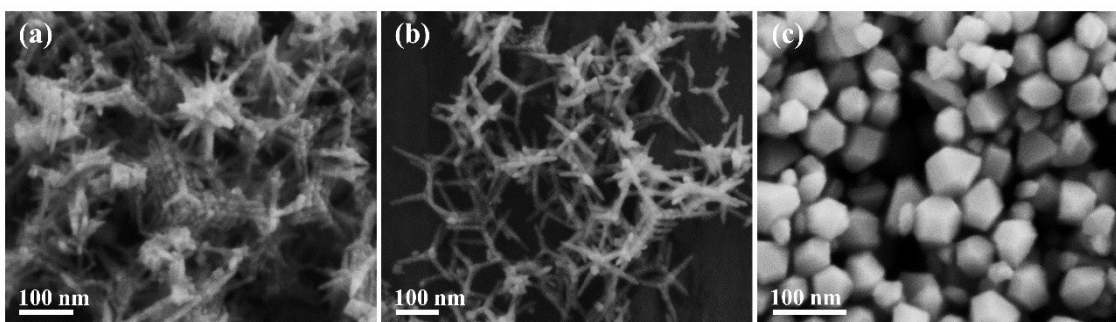


Fig. S4 SEM images of the samples prepared with different amounts of HCl: (a) 0 mL, (b) 0.05 mL, and (c) 0.2 mL.

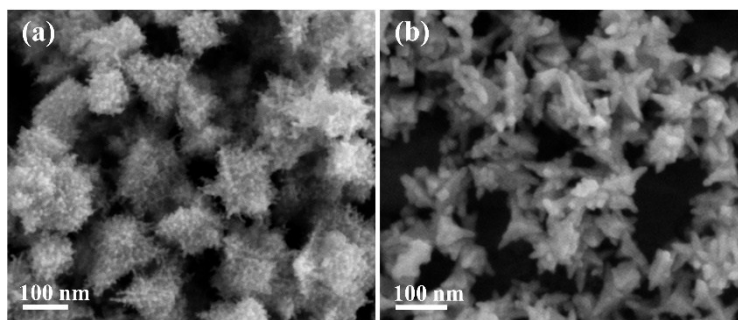


Fig. S5 SEM images of the samples prepared under the typical synthesis conditions with (a) 0 mg DM-970 and (b) 50 mg Brij58.

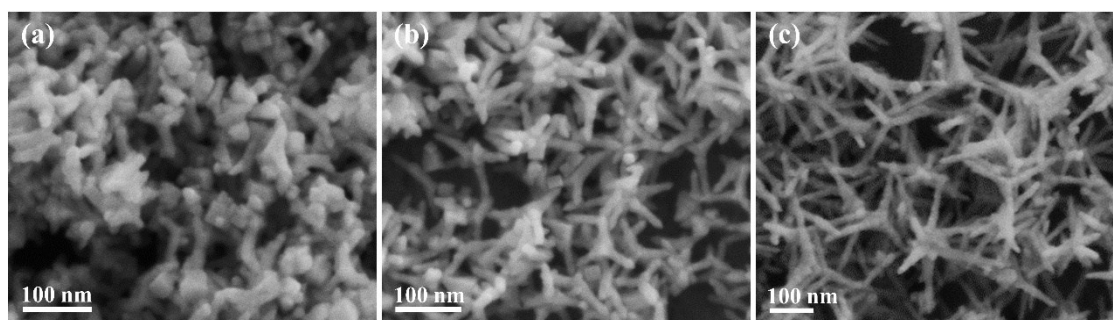


Fig. S6 SEM images of the PdRu TPs taken at different reaction times: (a) 10 min, (b) 30 min, and (c) 120 min.

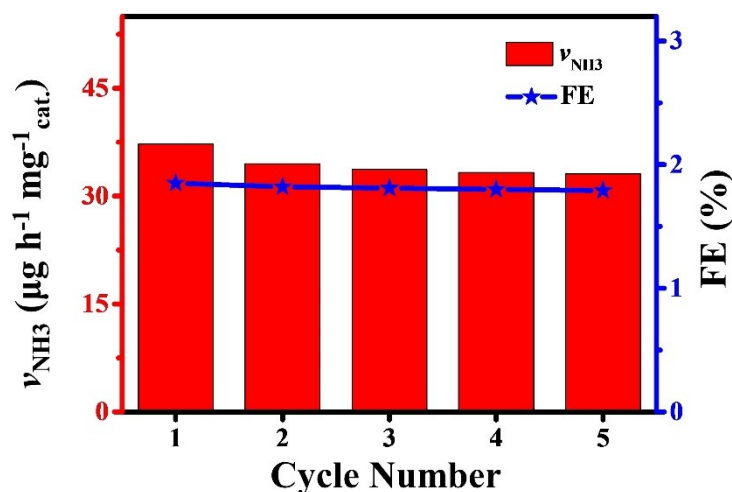


Fig. S7 Yield rate of NH_3 at the potentials of -0.2 V during the recycling tests.

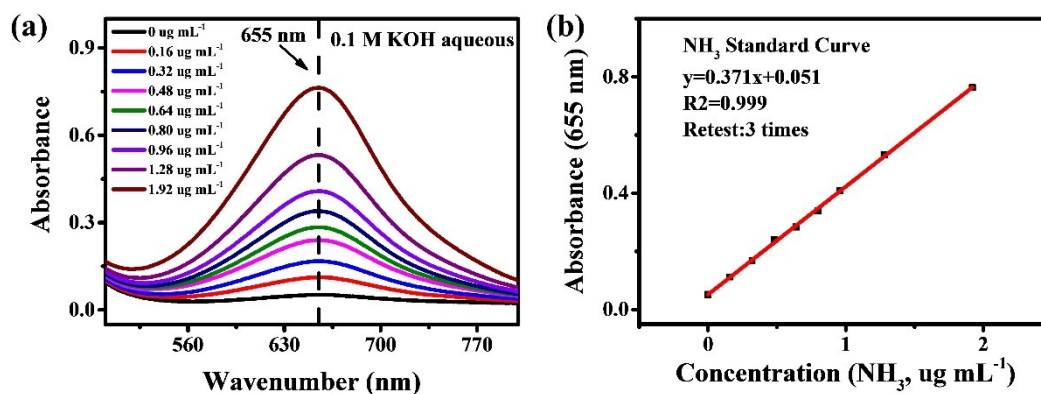


Fig. S8 Absolute calibration of the indophenol blue method using ammonium chloride solutions of known concentrations as standards. (a) UV–Vis absorption spectra of indophenol assays with NH_4^+ ions after incubation for 2 h at room temperature; (b) calibration curve used for estimation of NH_3 by NH_4^+ concentrations. The absorbance at 655 nm was measured by UV–Vis spectrophotometer, and the fitting curve shows good linear relation of absorbance with NH_3 concentrations ($y = 0.371x + 0.051$, $R^2 = 0.999$).

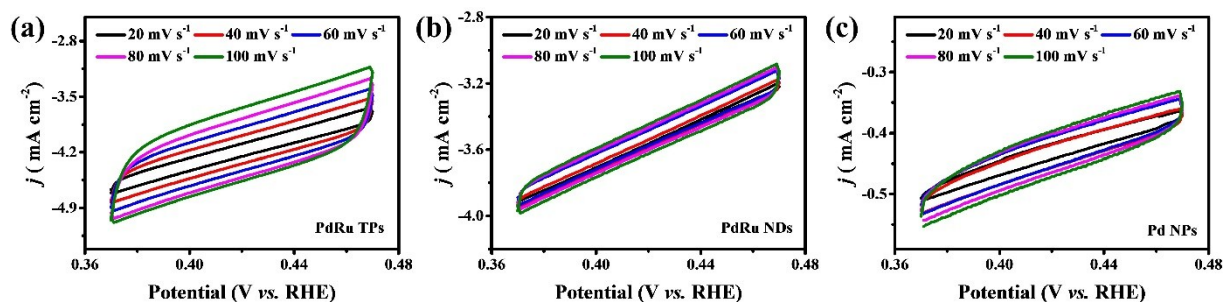


Fig. S9 cyclic voltammetry curves of different samples with various scan rates (20–100 mV s⁻¹) in the potential range of 0.37 to 0.47 V.

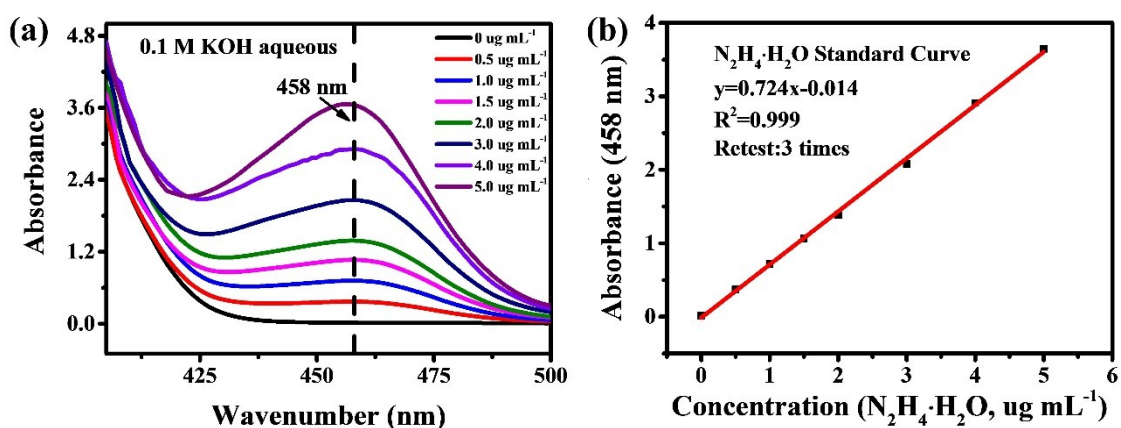


Fig. S10 Absolute calibration of the Watt and Chrisp (para-dimethylaminobenzaldehyde) method for estimating $N_2H_4 \cdot H_2O$ concentration, using $N_2H_4 \cdot H_2O$ solutions of known concentrations as standards. (a) UV-Vis absorption spectra of various $N_2H_4 \cdot H_2O$ concentration after incubation for 10 min at room temperature, (b) Calibration curve used for estimation of $N_2H_4 \cdot H_2O$ concentration. The absorbance at 458 nm was measured by UV-Vis spectrophotometer, and the fitting curve shows good linear relation of absorbance with $N_2H_4 \cdot H_2O$ concentrations ($y = 0.724x - 0.014$, $R^2 = 0.999$).

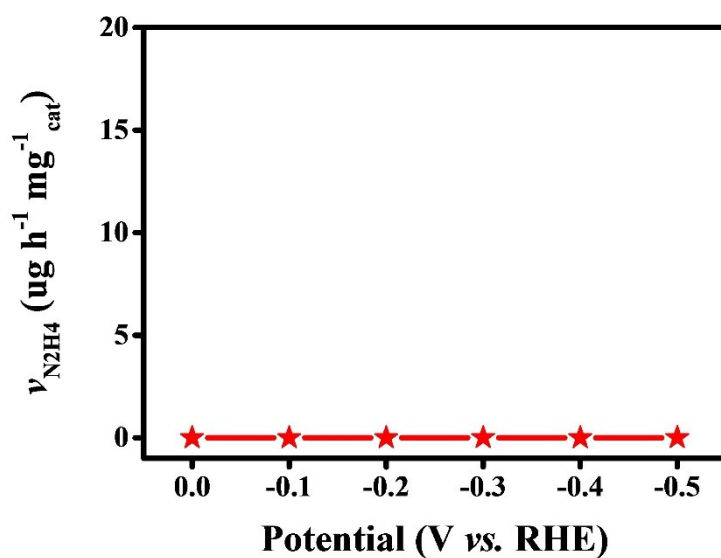


Fig. S11 Yield rate of N_2H_4 formation for the PdRu TPs at selected potentials.

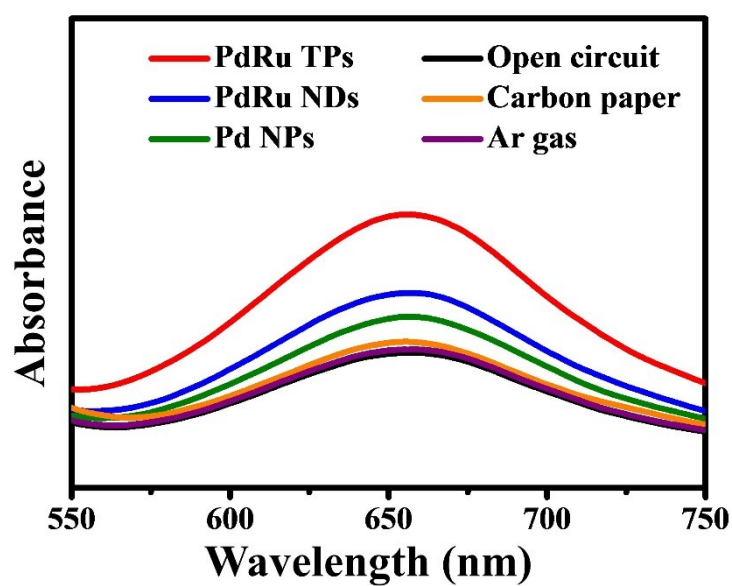


Fig. S12 UV-Vis absorption spectra of the KOH electrolyte stained with indophenol indicator after charging at -0.2 V for 2 h under various conditions.

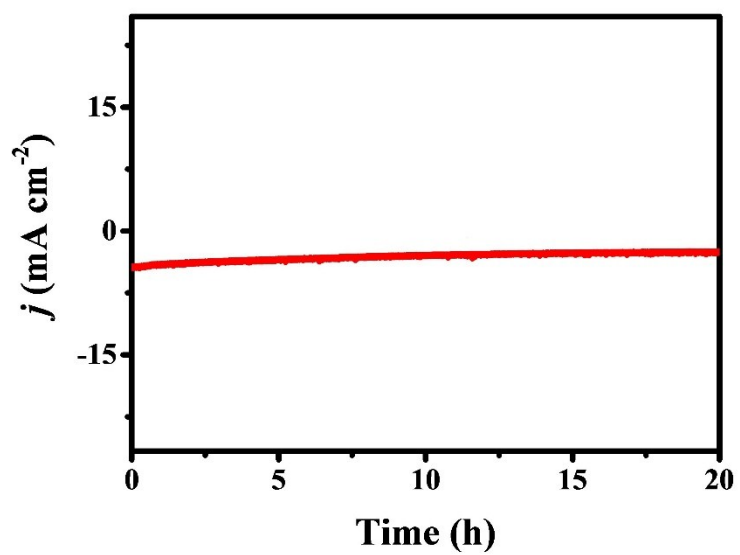


Fig. S13 Chronoamperometry curve of the PdRu TPs at the potential of -0.2 V for 20 h.

Table S1. Comparisons of the NRR yield on the different catalysts.

Catalysts	Electrolytes	Conditions	Yields	Ref.
PdRu TPs	0.1 M KOH	25 °C	37.23 $\mu\text{g h}^{-1} \text{mg}^{-1}_{\text{cat}}$ (11.9 $\mu\text{g h}^{-1} \text{cm}^{-2}$)	This work
Rh nanosheets	0.1 M KOH	25 °C	23.90 $\mu\text{g h}^{-1} \text{mg}^{-1}_{\text{cat}}$	1
Pd _{0.2} Cu _{0.8} /rGO	0.1 M KOH	25 °C	2.80 $\mu\text{g h}^{-1} \text{mg}^{-1}_{\text{cat}}$	2
C-ZIF-1100-1h	0.1 M KOH	25 °C	3.40 $\mu\text{g h}^{-1} \text{cm}^{-2}$	3
Au nanorods	0.1 M KOH	25 °C	1.65 $\mu\text{g h}^{-1} \text{cm}^{-2}$	4
Amorphous Bi ₄ V ₂ O ₁₁ /CeO ₂	0.1 M HCl	25 °C	23.21 $\mu\text{g h}^{-1} \text{mg}^{-1}_{\text{cat}}$	5
Au-TiO ₂	0.1 M HCl	25 °C	21.40 $\mu\text{g h}^{-1} \text{mg}^{-1}_{\text{cat}}$	6
a-Au/CeO _x -RGO	0.1 M HCl	25 °C	8.30 $\mu\text{g h}^{-1} \text{mg}^{-1}_{\text{cat}}$	7
Pd/C	0.1 M PBS	25 °C	4.90 $\mu\text{g h}^{-1} \text{mg}^{-1}_{\text{Pd}}$	8
Gold nanocages	0.5 M LiClO ₄	20 °C	2.35 $\mu\text{g h}^{-1} \text{cm}^{-2}$	9
PEBCD/C	0.5 M Li ₂ SO ₄	25 °C	1.58 $\mu\text{g h}^{-1} \text{cm}^{-2}$	10

References

1. H.-M. Liu, S.-H. Han, Y. Zhao, Y.-Y. Zhu, X.-L. Tian, J.-H. Zeng, J.-X. Jiang, B. Y. Xia and Y. Chen, *J. Mater. Chem. A*, 2018, **6**, 3211-3217.
2. M.-M. Shi, D. Bao, S.-J. Li, B.-R. Wulan, J.-M. Yan and Q. Jiang, *Adv. Energy Mater.*, 2018, **8**, 1800124.
3. S. Mukherjee, D. A. Cullen, S. Karakalos, K. Liu, H. Zhang, S. Zhao, H. Xu, K. L. More, G. Wang and G. Wu, *Nano Energy*, 2018, **48**, 217-226.
4. D. Bao, Q. Zhang, F.-L. Meng, H.-X. Zhong, M.-M. Shi, Y. Zhang, J.-M. Yan, Q. Jiang and X.-B. Zhang, *Adv. Mater.* 2017, **29**, 1604799.
5. C. Lv, C. Yan, G. Chen, Y. Ding, J. Sun, Y. Zhou and G. Yu, *Angew. Chem., Int. Ed.* 2018, **57**, 6073-6076.
6. M. M. Shi, D. Bao, B. R. Wulan, Y. H. Li, Y. F. Zhang, J. M. Yan and Q. Jiang, *Adv. Mater.* 2017, **29**, 1606550.
7. S. J. Li, D. Bao, M. M. Shi, B. R. Wulan, J. M. Yan and Q. Jiang, *Adv. Mater.* 2017, **29**, 1700001.
8. J. Wang, L. Yu, L. Hu, G. Chen, H. Xin and X. Feng, *Nat. Commun.*, 2018, **9**, 1795.
9. M. Nazemi, S. R. Panikkanvalappil and M. A. El-Sayed, *Nano Energy*, 2018, **49**, 316-323.
10. G. F. Chen, X. Cao, S. Wu, X. Zeng, L. X. Ding, M. Zhu and H. Wang, *J. Am. Chem. Soc.*, 2017, **139**, 9771-9774.